Genetics, Evolution, and Adaptive Significance of the Selfing Syndrome in the Genus *Capsella* ©W

Adrien Sicard,[a] Nicola Stacey,[b] Katrin Hermann,[b,1] Jimmy Dessoly,[b,2] Barbara Neuffer,[c] Isabel Bäurle,[a] and Michael Lenhard[a,3]

[a] Institut für Biochemie und Biologie, Universität Potsdam, D-14476 Potsdam-Golm, Germany
[b] Cell and Developmental Biology Department, John Innes Centre, Norwich NR4 7UH, United Kingdom
[c] Institut für Biologie, Universität Osnabrück, D-49076 Osnabrueck, Germany

The change from outbreeding to selfing is one of the most frequent evolutionary transitions in flowering plants. It is often accompanied by characteristic morphological and functional changes to the flowers (the selfing syndrome), including reduced flower size and opening. Little is known about the developmental and genetic basis of the selfing syndrome, as well as its adaptive significance. Here, we address these issues using the two closely related species *Capsella grandiflora* (the ancestral outbreeder) and red shepherd's purse (*Capsella rubella*, the derived selfer). In *C. rubella*, petal size has been decreased by shortening the period of proliferative growth. Using interspecific recombinant inbred lines, we show that differences in petal size and flower opening between the two species each have a complex genetic basis involving allelic differences at multiple loci. An intraspecific cross within *C. rubella* suggests that flower size and opening have been decreased in the *C. rubella* lineage before its extensive geographical spread. Lastly, by generating plants that likely resemble the earliest ancestors of the *C. rubella* lineage, we provide evidence that evolution of the selfing syndrome was at least partly driven by selection for efficient self-pollination. Thus, our studies pave the way for a molecular dissection of selfing-syndrome evolution.

INTRODUCTION

One of the most frequent evolutionary transitions in flowering plants is the change from reproduction by outbreeding to autogamous selfing, in which self-pollination and self-fertilization occur within the same flower (Stebbins, 1974; Barrett, 2002). The transition is often based on the breakdown of a genetic self-incompatibility system that prevents self-fertilization in the outbreeding ancestors (Busch and Schoen, 2008). In many cases, especially when the selfers are derived from animal-pollinated outbreeding taxa, this change in the reproductive system has been accompanied by a characteristic set of morphological and functional changes to the flower, termed the selfing syndrome (Darwin, 1876; Ornduff, 1969). Compared with their outbreeding sister taxa, autogamous selfers generally have smaller flowers that open less and have a shorter distance and reduced temporal separation between dehiscing anthers and receptive stigmas, they produce relatively less pollen, and they also produce less

scent and nectar. These concerted changes have evolved hundreds of times independently among the angiosperms (Barrett, 2010). Thus, they represent an ideal model for addressing a number of basic questions about the genetics of adaptation and morphological evolution in plants (Sicard and Lenhard, 2011). These include the following: Which parameters of growth and development have been changed to bring about altered morphologies? Mutations in how many genes are involved in the evolution of individual traits?

The developmental changes that underlie different flower sizes in outbreeding versus selfing taxa fall into two general patterns. Either the duration of flower growth has been strongly reduced in the selfer with a concomitant increase in the rate of growth, leading in sum to smaller flower organs (e.g., in *Clarkia xantiana*, *Mimulus*, or *Limnanthes*) (Guerrant, 1988; Fenster et al., 1995; Runions and Geber, 2000) or a substantially reduced rate of growth has caused the decrease in flower size despite a prolonged period of growth, such as seen in *Arenaria uniflora* (Hill et al., 1992). These different patterns are thought to reflect, in part, different ecological scenarios that have driven the evolution of the selfing lineage (Runions and Geber, 2000).
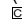
The genetic basis of the selfing syndrome has been studied using quantitative genetic approaches in three different genera, *Mimulus*, *Leptosiphon*, and *Solanum* (*Lycopersicon*) (Bernacchi and Tanksley, 1997; Lin and Ritland, 1997; Fishman et al., 2002; Georgiady et al., 2002; Goodwillie et al., 2006). In general, a moderate to large number of quantitative trait loci (QTL) affect individual floral traits, each with small to moderate effects. However, for several traits, especially for traits likely to be causally linked to increased selfing, such as reduced anther-stigma
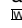
separation, major-effect QTL have been detected that explain up to 50% of the phenotypic variance. QTL mapping has also indicated that many of the identified loci affect more than one trait, such as corolla width and anther-stigma separation (Fishman et al., 2002). When comparing the results of mapping studies using closely related pairs of species (e.g., in the genus *Solanum*), comparable trait changes appear to have been brought about by changes to different genomic loci (Bernacchi and Tanksley, 1997; Georgiady et al., 2002). The molecular basis of a QTL influencing a selfing-syndrome trait has only been defined in one case: a regulatory mutation in a gene encoding a basic helix-loop-helix–related protein is responsible for the reduced style length and, thus, reduced anther-stigma separation in domesticated versus wild tomatoes (*Solanum lycopersicum* versus *Solanum pennellii*) (Chen et al., 2007).

A better understanding of selfing-syndrome evolution will require isolating the causal genes that contribute to trait variation. The genus *Capsella* Medikus (Brassicaceae) has recently been highlighted as a promising model to facilitate this task of identifying the molecular polymorphisms underlying the morphological changes in the selfing syndrome (Foxe et al., 2009; Guo et al., 2009). This genus is a member of the mustard family and together with the genetic model species *Arabidopsis thaliana*, it belongs to the tribe of Camelineae (German et al., 2009). Of the two diploid species in this genus, *Capsella grandiflora* shows a typical sporophytic self-incompatibility as found in other *Brassicaceae* and reproduces by outbreeding (Paetsch et al., 2006, 2010), whereas the red shepherd's purse (*Capsella rubella* Reuter) is self-compatible and reproduces predominantly by autogamous selfing (Hurka and Neuffer, 1997). This difference in the reproductive system is linked to a strongly reduced flower size in the selfing *C. rubella* compared with *C. grandiflora*, and this contrast is in fact one of the main taxonomic criteria for distinguishing the two species (Hurka and Neuffer, 1997; Foxe et al., 2009). *C. rubella* was derived from *C. grandiflora* via a severe population bottleneck, with potentially only one self-compatible diploid individual giving rise to the entire present *C. rubella* lineage (Foxe et al., 2009; Guo et al., 2009), and the divergence time of the two species has been estimated at 20,000 to 50,000 years ago (Foxe et al., 2009; Guo et al., 2009), whereas the *Capsella* and *Arabidopsis* lineages are thought to have diverged ~10 to 14 million years ago (Koch and Kiefer, 2005). Whereas *C. grandiflora* is restricted to the Western Balkans and Northern Italy, the geographical distribution of *C. rubella* includes most of the Mediterranean climatic regions of the world except South Africa (Paetsch et al., 2010). The dating of the divergence together with the different geographical distributions have led to the suggestion that the evolution of selfing in *C. rubella* was driven by selection for reproductive assurance in the pollinator-limited conditions during the recolonization of Southern and Central Europe after the last ice age (Foxe et al., 2009; Guo et al., 2009). This suggestion is consistent with the more general scenario that the transition to selfing should be favored at the margins of a species' distribution where conspecifics and/or pollinators are scarce, as under these conditions the benefit of assured reproduction could outweigh the costs of genetic inbreeding (Darwin, 1876; Stebbins, 1950; Baker, 1955; Lloyd, 1992). Importantly, their recent divergence and resulting close relationship suggest that *C. grandiflora* and *C. rubella* should be easily amenable to genetic analysis, including the cloning of individual selfing-syndrome genes (Hurka and Neuffer, 1997; Foxe et al., 2009).

Thus, the aims of the studies reported here were (1) to quantify the phenotypic variation in the flowers of *C. grandiflora* and *C. rubella* and describe its developmental basis; (2) to address the genetic basis of floral variation; and (3) to ask which adaptive advantage could be conferred by the modified flower morphology in the selfing lineage. To study the genetics of the selfing syndrome, we established a population of recombinant inbred lines (RILs) derived from an interspecific cross between *C. grandiflora* and *C. rubella.* This population of RILs should also be useful for studying other aspects of phenotypic variation within this genus.

RESULTS

Morphological Differences between Flowers of the Outbreeder *C. grandiflora* and the Derived Selfer *C. rubella*

To characterize the evolution of floral features in the genus *Capsella*, we quantified variation in floral traits between *C. rubella* and *C. grandiflora* and asked whether any phenotypic differences are fixed between the two species. We grew in parallel five individuals each of nine accessions of *C. grandiflora* and 15 accessions of *C. rubella* and measured various floral and vegetative traits. All of the *C. grandiflora* accessions were originally collected in the species' main region of distribution in Greece, whereas the *C. rubella* accessions originated from a much wider geographical range of locations (see Supplemental Table 1 online), reflecting the extensive geographical spread of *C. rubella* compared with the ancestral lineage.

The overall growth habit of the two species is very similar (see Supplemental Figure 1A online). However, all *C. rubella* accessions form much smaller flowers than any of the *C. grandiflora* accessions, with an 85% reduction in the average area of petals (Figure 1A, Table 1; see Supplemental Figure 1B online), suggesting that the reduced flower size is fixed in the *C. rubella* compared with the *C. grandiflora* lineage. By contrast, the size of the seventh leaf did not differ significantly between the two species (Figure 1B), indicating that the reduction in size was specific for floral organs. At the cellular level, we did not detect a significant difference in the size of petal epidermal cells when comparing a representative accession for each species (Figure 1D), suggesting that the difference in overall petal size is due to different numbers of petal cells. To determine the developmental basis for the reduced petal size in *C. rubella*, we followed growth of petal primordia in a representative accession of each of the two species over time (Figure 1C). Whereas the initial rate of petal growth is very similar between *C. rubella* and *C. grandiflora* flowers, petals of *C. rubella* cease growing sooner than those of *C. grandiflora*, indicating that the difference in final cell number and petal size results from a premature termination of proliferation and petal growth in *C. rubella* flowers. This shortened growth phase does not reflect a plant-wide abbreviation of developmental phases, as, for example, the studied *C. rubella* accession flowered roughly 10 d later than the *C. grandiflora* accession (see Supplemental Figure 2A online).

Table 1. Quantitative-Genetic Parameters for Morphological Traits

Trait	C. grandiflora (Cg926)	C.rubella (Cr1504)	Mean RILs	Min RILs	Max RILs	H^2	Vg	Ve	CVg
Leaf area (cm²)	6.51 ± 1.84	6.33 ± 1.87	7.18 ± 2.53	2.07	13.44	0.67778308	5.858594	2.663185	33.71
Leaf length (cm)	8.20 ± 1.5	9.46 ± 1.40	8.620 ± 2.00	4.0	13.12	0.70829790	3.687092	1.438308	22.25
Leaf width (cm)	1.92 ± 0.37	2.03 ± 0.22	2.01 ± 0.36	1.03	2.76	0.67001842	0.116922	0.055037	17.03
Petal area (mm²)	8.41 ± 1.98	1.29 ± 0.33	3.29 ± 0.88	1.73	6.09	0.70638043	0.693963	0.242718	25.25
Petal length (mm)	4.43 ± 0.43	2.03 ± 0.31	3.00 ± 0.37	2.16	4.11	0.60957321	0.123187	0.069917	11.68
Petal width (mm)	3.01 ± 0.47	1.05 ± 0.14	1.77 ± 0.25	1.22	2.66	0.68773508	0.060007	0.023296	13.77
Distance anthers-stigma (cm)	1.66 ± 0.17	0.71 ± 0.14	1.27 ± 0.226	0.7	1.83	0.40419300	0.038366	0.05406	15.42
Petal opening angle	55.33 ± 5.82	34.58 ± 4.72	57.51 ± 9.72	31.08	80.89	0.48367054	74.108000	73.210000	14.97
Selfing efficiency (%)	n.a.	74 ± 6	60.66 ± 20.54	10.34	93.02	0.38326000	325.272764	522.300000	29.73

Vg, among-RILs (genetic) variance; Ve, residual (environmental) variance; CVg, coefficient of genetic variance (see Methods); max, maximum value; min, minimal value, H^2, broad-sense heritability; n.a., not applicable.

In addition to differences in petal size, flowers of *C. rubella* also show other modifications relative to those of *C. grandiflora*. Whereas flowers of *C. grandiflora* open very widely throughout the course of the day, with strongly reflexed petals, *C. rubella* flowers stay much more closed (Figure 2A). This is evident when quantifying the angle between the longitudinal axis of the gynoecium and the stalks of the petals across the different *C. rubella* and *C. grandiflora* accessions. This petal opening angle is reduced from 55° in *C. grandiflora* to 35° in *C. rubella* (Figure 2C, Table 1). Concomitantly, the distance between the stigma and the dehiscing anthers is reduced by 57% in *C. rubella* (0.71 mm compared with 1.66 mm in *C. grandiflora*; Figure 2B, Table 1). This is likely the combined result of both a reduced opening angle between the gynoecium and the stamen filaments and a reduction in the absolute length of stamens and the gynoecium. The ratio between the total lengths of the gynoecium and of the long anthers does not differ between the two species (Figure 2D). We also found that the number of pollen grains per flower is reduced by ∼75%, whereas the number of ovules per gynoecium is increased by almost 1.5-fold in *C. rubella* compared with *C. grandiflora*, leading to a pollen-to-ovule ratio per flower in the selfing lineage that is only 17% of the value of the outbreeder (see Supplemental Figures 2B and 2C online).

Thus, in summary, flowers of *C. rubella* show many of the trait changes that are typically found in selfing lineages compared with their ancestral outbreeding lineages, with reductions in the size of petals, the opening angle of the petals, the distance between stigma and anthers, and the pollen-to-ovule ratio in the selfer. The trait differences appear fixed between the two species, suggesting that the modifications in flower morphology occurred after the divergence of the two lineages.

Construction of an Interspecific RIL Population

To initiate a genetic analysis of the selfing syndrome, we crossed a representative *C. grandiflora* (Cg926) accession with a representative *C. rubella* (Cr1504) accession, with *C. grandiflora* as the maternal parent. From the F1 population, we selected a single, self-compatible individual and harvested F2 seeds derived from selfing. Traits of interest, such as petal size, varied continuously in the F2 population (data not shown; cf. below for values from an independent F2 population). Thus, we decided to propagate the

hybrid individuals through six additional generations via selfing and single-seed descent to establish a population of RILs for mapping QTL that contribute to the trait differences between the parental species.

We established a total of 152 RILs, of which 142 were used for genotyping, phenotyping, and subsequent QTL mapping. To establish a genetic map of the RIL population, we generated 97 PCR-based markers by identifying sequence polymorphisms between the two parental strains segregating in the recombinant population (see Supplemental Tables 2 and 3 online). Marker establishment was in part guided by the published genetic map of *Capsella* and by the known relationship between blocks of the *Arabidopsis* genome and the ancestral karyotype within the *Brassicaceae* that appears to be a good model for the *Capsella* genome (Boivin et al., 2004; Schranz et al., 2006). Essentially all of the markers are located within predicted protein-coding genes, facilitating comparisons of synteny between the resulting map of the RIL population and the *Arabidopsis* genome. After genotyping the 142 RILs with the 97 markers, we established a genetic map using a logarithm of odds (LOD) score threshold of 3.5 or higher, resulting in eight linkage groups (Figure 3) representing chromosomes A to H as predicted from previous analyses (Boivin et al., 2004). The map spans a total genetic distance of 524 centimorgans (cM). The average distance between markers is 5.45 cM, with a maximum distance of 17 cM and an average of 12 markers (minimum 8 and maximum 16 markers) per linkage group. The linkage map obtained is consistent with the results by Boivin et al. (2004) regarding the synteny between *Arabidopsis* and *Capsella* (see Supplemental Table 3 online).

Analysis of the genetic structure of the RIL population revealed four regions with clear segregation distortion (i.e., a predominance of *C. rubella* alleles) (see Supplemental Figure 3A online). One of these regions (at the bottom end of chromosome G) contains the *Capsella* S-locus, with plants homozygous for the *C. grandiflora* alleles showing self-incompatibility (see Supplemental Figure 3B online). Analyzing recombination break points localized the functional S-locus between markers G06 and G06.5 (see Supplemental Figure 3B online). These two markers represent the *Capsella* homologs of the *Arabidopsis* loci At4g23713 and At4g19300, respectively. The region between these loci in the *Arabidopsis* genome contains the *S-locus receptor kinase* gene At4g21370 and the neighboring gene for S-locus Cys-rich
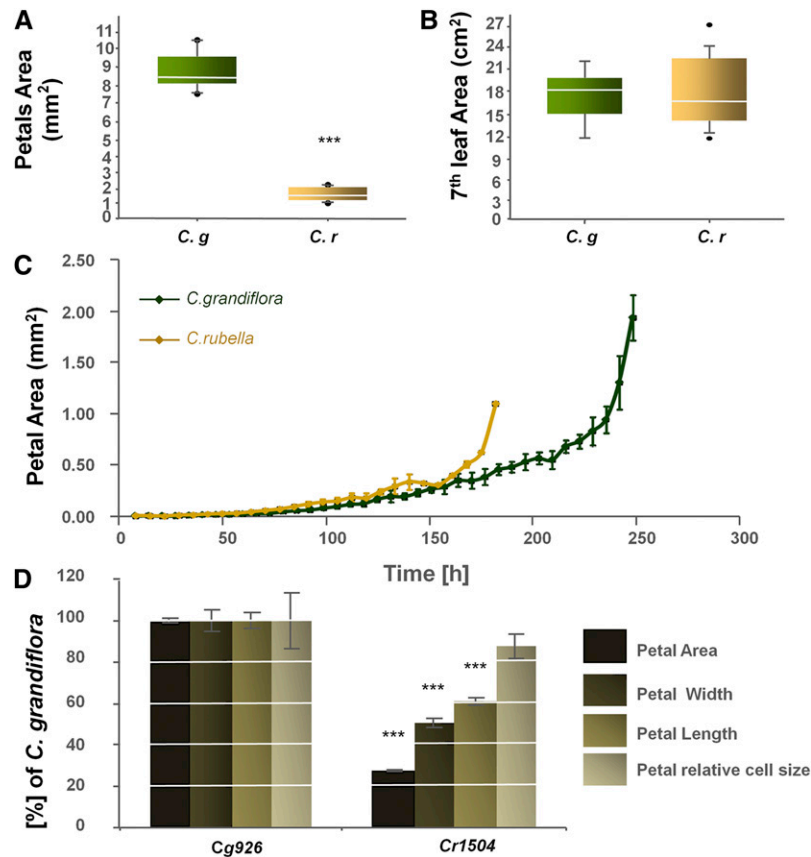
Figure 1. Organ Size Phenotypes of *C. grandiflora* versus *C. rubella*.

(A) Average petal areas of nine *C. grandiflora* and 15 *C. rubella* accessions. Box plots in this and all following graphs show the median value (white line), the 25 and 75 percentiles (bottom and top bounds of the box, respectively), the top and bottom inner fences (whiskers; top inner fence is defined as the upper quartile plus 1.5 times the interquartile range, or the maximum value, if that is smaller; the bottom inner fence is defined analogously), and any outliers (dots).

(B) Average leaf areas of nine *C. grandiflora* and 15 *C. rubella* accessions.

(C) Growth of petal primordial in a representative accession each of *C. grandiflora* (Cg926) and *C. rubella* (Cr1504). Petal growth was followed starting from the youngest petals that could be manually dissected to petals of flower buds just prior to bud opening. Petal primordia in *C. rubella* grow at the same initial rate but stop growing earlier than those of *C. grandiflora*. Values are means ± SE for two petals from four flowers per time point.

(D) Petal dimensions and petal cell sizes from a representative accession each of *C. grandiflora* (Cg926) and *C. rubella* (Cr1504). Values are means ± SE for four (area, length, and width) or three petals (cell size) expressed relative to the *C. grandiflora* values.

Asterisks indicate statistically significant differences from *C. grandiflora* as determined by a Student's *t* test at $P < 0.05$ (*), $P < 0.01$ (**), and $P < 0.001$ (***).

protein. Assuming that this chromosomal region is essentially syntenic between *Capsella* and *Arabidopsis*, this mapping result suggests that loss of self-incompatibility in *C. rubella* is associated with a loss-of-function mutation in the canonical Brassicaeceae S-locus. A second region with distorted segregation at the top end of chromosome A carries a recessive mutation from the *C. grandiflora* parent that causes a pale green phenotype, slow growth, and severely reduced fertility when homozygous (see Supplemental Figure 3C online). Selection for self-fertility and against the recessive pale green mutant phenotype can therefore explain the biased representation of these two chromosomal regions in the RIL population. However, we have not detected an obvious phenotype that could account for the distorted segregation on chromosomes B and C.

Heritability and Phenotypic Correlations

We phenotyped the RIL population for leaf area (LA), leaf length (LL), leaf width (LW), petal area (PA), petal length (PL), petal width (PW), petal opening angle (POA), and the distance between the anthers and the stigma (DAS) by measuring 10 (leaf- and petal-size traits) or five (opening angle and anther-stigma distance) individuals per line, respectively, and using the average value as an estimate for the phenotype of each line. We also estimated the efficiency of self-pollination for 46 of the RILs by calculating the ratio between the number of seeds formed by unmanipulated flowers and the number of seeds formed after manual self-pollination of flowers. The broad-sense heritability for the morphological traits ranged from 0.40 for DAS to 0.71 for PA and LL
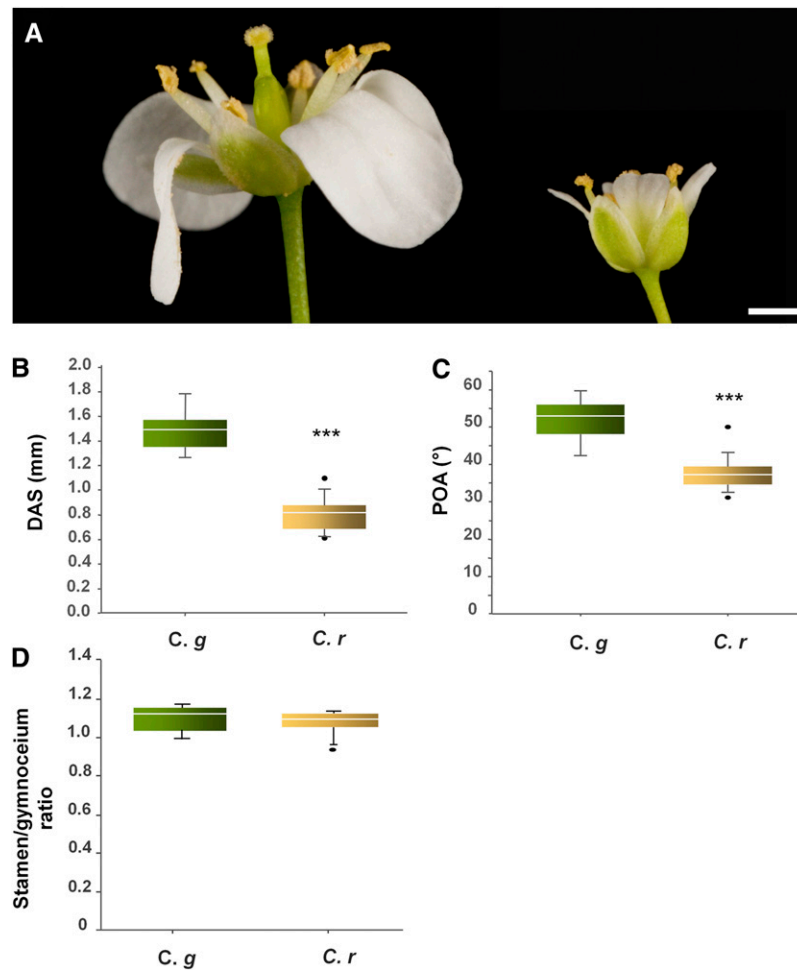
Figure 2. Flower Opening in *C. grandiflora* versus *C. rubella*.

(A) Lateral views of mature *C. grandiflora* (left) and *C. rubella* flowers (right), showing the difference in the extent of flower opening. Bar = 1 mm.
(B) Distance between anthers and stigma (DAS) in nine *C. grandiflora* and 15 *C. rubella* accessions.
(C) Petal opening angle (POA) in nine *C. grandiflora* and 15 *C. rubella* accessions.
(D) Ratio between the lengths of the gynoecium and that of the long stamens in nine *C. grandiflora* and 15 *C. rubella* accessions.
Symbols in box plots for **(B)** to **(D)** as in Figure 1A. Asterisks indicate statistically significant differences from *C. grandiflora* as determined by a Student's *t* test at P < 0.05 (*), P < 0.01 (**), and P < 0.001 (***).
[See online article for color version of this figure.]

(Table 1), with the heritability for the selfing efficiency slightly lower at 0.38, indicating that all of the studied traits have a strong genetic basis. All of the leaf traits showed strong transgressive segregation compared with the parental strains of the RIL population (Table 1; see Supplemental Figure 4 online).

Transgressive segregation (i.e., the appearance of more extreme phenotypes than in either of the parents) can either be due to the parents harboring both positively and negatively acting alleles that become recombined in more extreme combination in the hybrids or to overdominance when heterozygotes at a locus show higher or lower phenotypes than either of the alternative homozygotes. However, as in our RILs essentially all of the genome is homozygous, the latter explanation seems unlikely. LA and LW were normally distributed, whereas three of the four

tests used indicated a deviation from normality for LL (see Supplemental Table 4 online). There was no evidence for transgressive segregation for any of the petal size traits, and PA values were shifted away from the mid-parental value to smaller sizes (Table 1; see Supplemental Figure 4 online); whereas PL and PW were normally distributed, the distribution for PA deviated from normality. After log transformation, PA was normally distributed (see Supplemental Table 4 online). Also, DAS, POA, and ASE were all normally distributed (see Supplemental Table 4 online), with all three parameters showing transgressive segregation toward higher values (Table 1; see Supplemental Figure 4 online).

To determine whether the shift in PA values toward smaller sizes reflected a dominant action of small-petal alleles from the
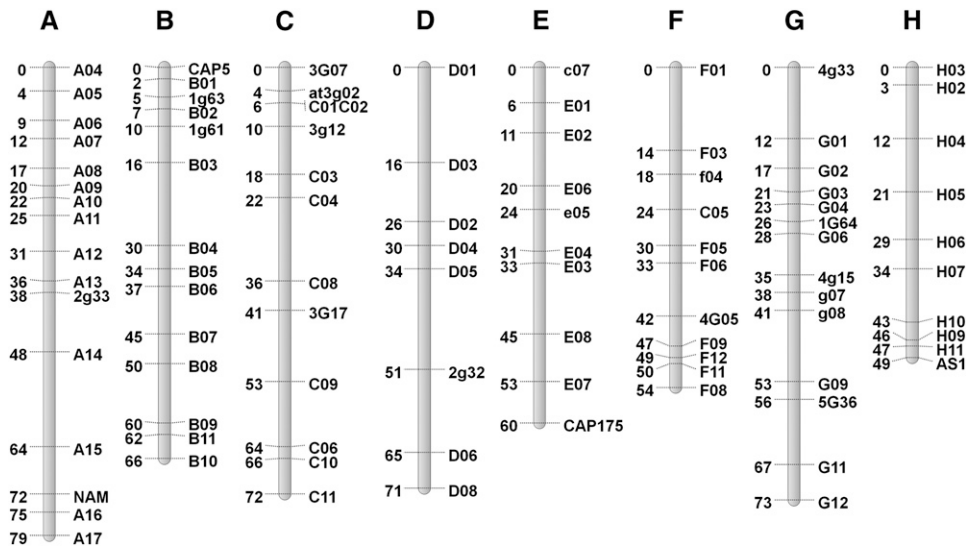
Figure 3. Genetic Map of the *C. grandiflora* × *C. rubella* RIL Population.

Individual linkage groups are shown by gray bars. Names of the markers used are given to the right of each linkage group, and each genetic position in centimorgans is shown to the left.

C. rubella parent, we measured petal size of F1 plants from a cross of the two parental strains of the RIL population (see Supplemental Figure 5 online). Petal size of the F1 individuals was even somewhat higher than the mid-parental value, arguing against dominance of *C. rubella* petal-size alleles. Rather, we suggest that distorted segregation of petal-size QTL linked to the regions on chromosomes A, C, and G that show enrichment for the *C. rubella* alleles in the RIL population (see below and above) can explain the shift of PA values to smaller sizes.

To determine whether the differences in the various traits are under independent genetic control, we calculated genetic correlations among the traits in our population (Figure 4). Not surprisingly, the three leaf parameters (LA, LL, and LW) showed strong positive correlations, as did the three petal-size parameters PA, PL, and PW (Figure 4). Whereas the correlation between area and length or width of an organ is trivial, the strong positive correlations between LL and LW, as well as between PL and PW, suggest that variation in overall organ size is largely due to functionally different alleles at loci that act on overall organ growth, rather than specifically on organ length or width. By contrast, leaf traits were not correlated with petal traits, indicating that variation in the size of vegetative and floral organs has an independent genetic basis. DAS was positively correlated not only with the opening angle of the petals, but also with petal size. The latter correlation is probably due to an underlying positive correlation between petal size and stamen length, as for a given opening angle, DAS will necessarily increase with increasing length of the gynoecium and stamens. By contrast, petal size and opening angle were not directly correlated (Figure 4). In summary, variation in the size of leaves and petals and in other aspects of floral morphology, such as the petal opening angle, appears to have a largely independent genetic basis, thus suggesting independent evolution of the different traits.

QTL Mapping

We used the information about the phenotypes and the genotypes of our RILs to localize QTL influencing variation in the measured traits, using multiple QTL mapping. Permutation analysis (10,000 replications) was used to determine 5% significance thresholds for the individual traits. LOD score peaks on the same linkage group were interpreted as representing different QTL if the 2-LOD confidence intervals of the peaks did not overlap. Results of the QTL mapping are presented in Figure 5 and Table 2. For LA, LL, and LW, one significant QTL was detected on chromosome B, explaining 11, 17, and 16.6% of the total phenotypic variance for the respective trait. For PA, we found six QTL (PAQTL_1 to PAQTL_6; log-transformed values of PA were used to account for the non-normality of the untransformed values). Of these, PAQTL_4 and PAQTL_5 were both located on chromosome F, whereas the remaining QTL were each found on a separate chromosome. Five of the six QTL for PA (PAQTL_1, 2, 4, 5, and 6) had a major effect (following the definition by Tanksley, 1993), explaining 11.6, 10.6, 15.5, 17.6, and 16.8% of the total genetic variance under the full QTL model, respectively. Similarly, six QTL each were detected for PL and PW. Comparing the locations of the QTL for PA, PL, and PW indicates that PAQTL_3 influences only the width and PAQTL_5 mainly influences the length of the petals, suggesting that these two QTL reflect variation in genes that specifically act on either of the linear dimensions of petals. Of the six QTL detected for PL, only one (PLQTL_2) does not overlap with a QTL for PA; similarly, of the six QTL for PW, the only one that does not overlap with a QTL for PA was the very weak PWQTL_4 at the end of chromosome C. Three QTL were identified as influencing DAS. Of these, DASQTL_1 and 2 overlap with the QTL for petal opening POAQTL_1 and POAQTL_2. The strongest effect on DAS and POA is from the
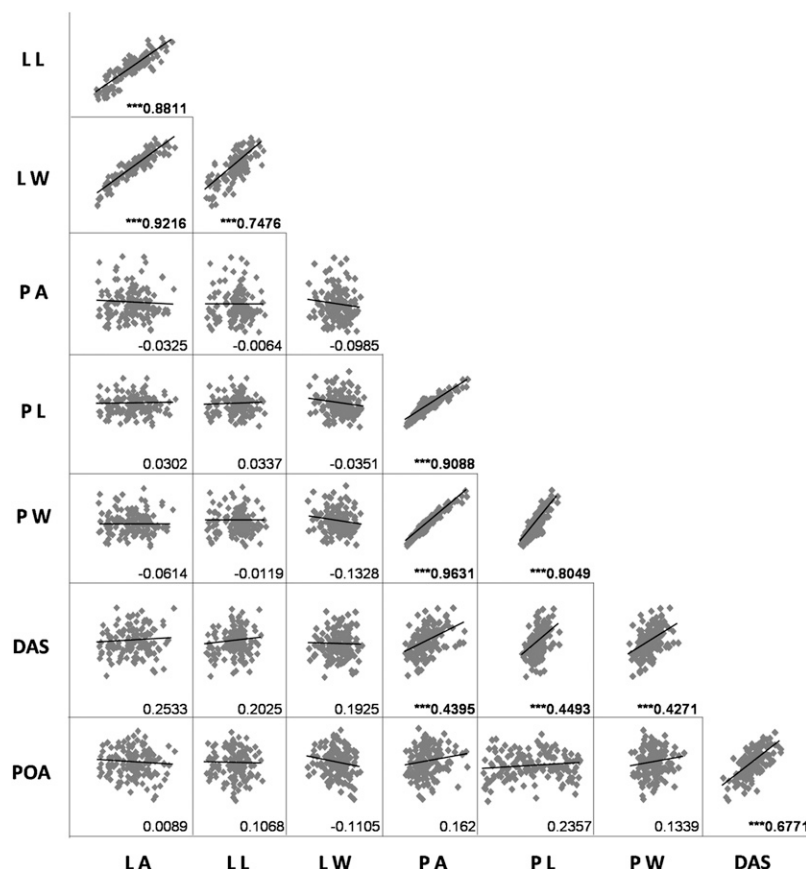
Figure 4. Genetic Correlations between Leaf and Floral Traits in the *C. grandiflora* × *C. rubella* RIL Population.

Correlation plots of the indicated phenotypic parameters measured in the RIL population. For each pairwise comparison, dots represent individual RILs, and dark line represents the linear regression line. Values below each plot are Pearson's correlation coefficients (*r*), with significant correlations indicated by bold type and asterisks (***P < 0.01).

joint QTL on chromosome D, explaining 23.3% of the total phenotypic variance for POA. The confidence interval for the weak DASQTL_1 on chromosome B overlaps with that for PAQTL2 and PLQTL3, possibly reflecting the positive correlation between petal size and DAS. Also, the weak POAQTL3 overlaps with PLQTL5.

We compared the results of our QTL mapping to the estimated power of our study (Sen et al., 2007) using PA and POA as example traits. Given the calculated genetic and environmental variances for these traits, the size of the RIL population, and the number of replicates per line, for a QTL to be detectable with a power of 90%, it would have to explain 19% or more of the total phenotypic variance for PA and POA. This correlates well with the estimated effects of the identified POAQTL, whereas none of the PAQTL had effects this strong, suggesting that additional PAQTL were likely missed due to the limited power. Accordingly, the combined estimated effects of the three POAQTL could explain all of the difference in flower opening between the two parental strains, whereas the combined effects of the QTL for PA, PL, PW, and DAS accounted for just over half of the difference between the parents (56.7, 67.5, 55.1, and 52.6%, respectively). Therefore,

petal size and DAS appear to be influenced by additional QTL segregating in the RIL population that were not detected here.

Thus, variation in the typical selfing-syndrome traits between the two *Capsella* species has a complex genetic basis and results from the accumulation of several mutations at different loci in the genome. Petal size has evolved in an organ-specific manner, as none of the QTL influencing petal traits also affects the size of leaves. Although a main QTL for DAS and POA was detected, variation in these two traits is also due to allelic differences at several loci.

History of Selfing-Syndrome Evolution

As described above, the geographical distribution of *C. rubella* by far exceeds that of the ancestral *C. grandiflora*. The close relatedness of the different *C. rubella* accessions demonstrated by population-genetic analyses strongly suggests that *C. rubella* spread geographically after the breakdown of self-incompatibility in one or a few individuals of a *C. grandiflora*–like ancestor in Greece (Foxe et al., 2009; Guo et al., 2009). Our finding that the reduced size of the petals is fixed in all tested *C. rubella*
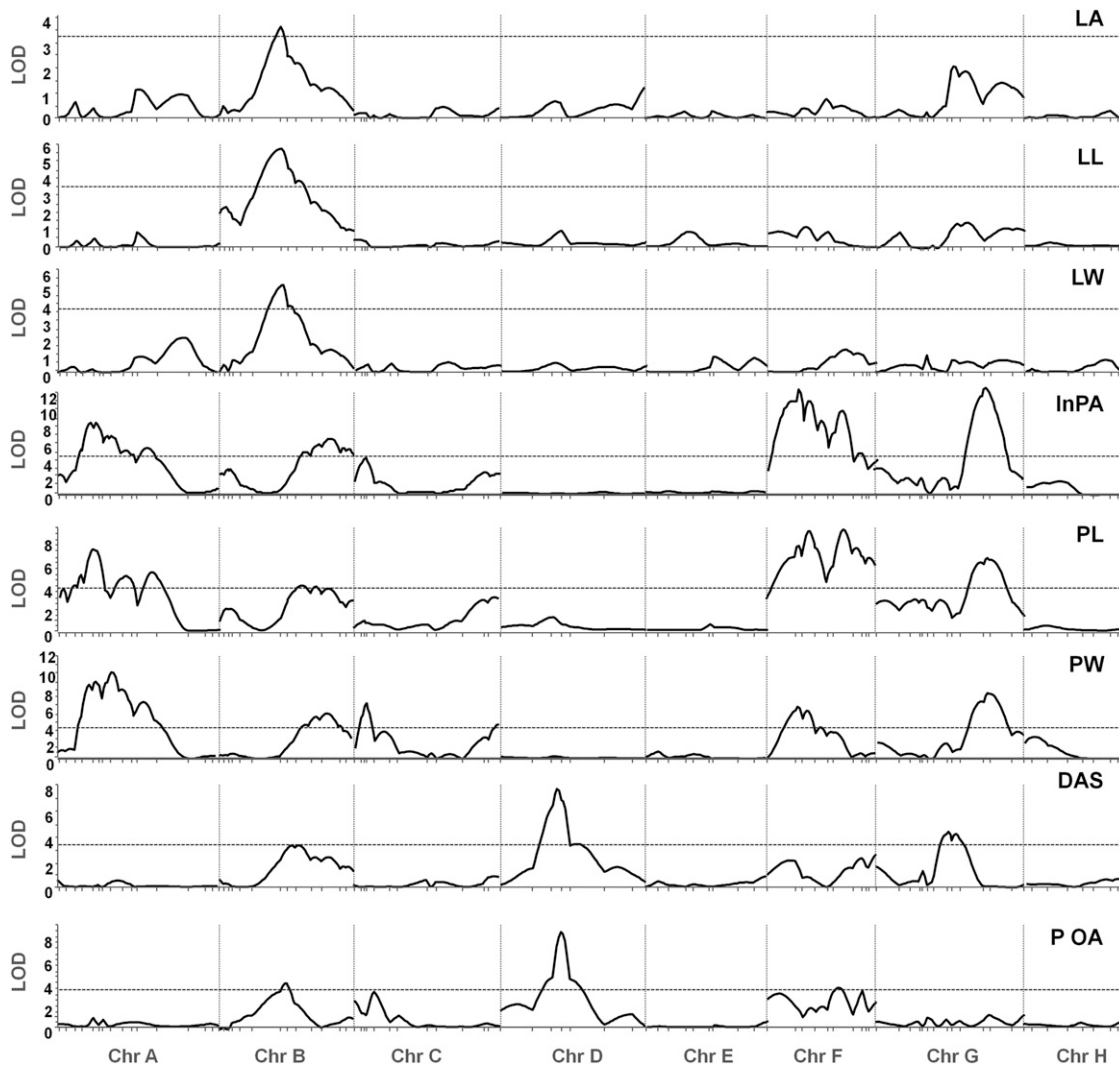
Figure 5. Location of QTL Affecting Leaf and Flower Phenotypes.

LOD score plots are shown for each of the traits indicated on the right. The horizontal dashed lines indicate the significance threshold (P < 0.05) as determined by permutation testing. The vertical dashed lines delimit linkage groups A to H; ticks below the *x* axes show the positions of individual genetic markers. lnPA, ln-transformed petal area; other abbreviations are as in Figure 4.

accessions (see above) raises the question of when petal size was altered relative to the geographical spread of *C. rubella*. Two extreme scenarios are conceivable: The selfing-syndrome may have evolved very quickly after the transition to self-compatibility and before the geographical spread; alternatively, flower size may have been reduced independently in different populations after the geographical spread of a form with large, *C. grandiflora*–like flowers. Under the first scenario, all current *C. rubella* accessions would be predicted to share the same small flower alleles, whereas independent evolution in local populations may have always affected the same genetic loci or have involved changes to different loci.

To gain a first insight into this question, we analyzed phenotypic segregation in crosses of two different *C. rubella* accessions, Cr1377 from Argentina and Cr1504 from Tenerife, which

have previously been shown to belong to two only distantly related lineages of *C. rubella* (Foxe et al., 2009). If the reduction in flower size involves the same loci in both accessions, an F2 population should not show transgressive segregation, but rather produce the same phenotypic distribution as the two parental strains; by contrast, the involvement of different loci in the two *C. rubella* accessions should lead to transgressive segregation in the hybrid progeny. As controls, we also analyzed the phenotypic distribution in the F2 of a cross between Cr1377 and the *C. grandiflora* accession Cg926, as well as in the F8 population of our RILs derived from the Cr1504 × Cg926 cross (Figure 6; see Supplemental Table 5 online).

Both *C. rubella* parental accessions showed a very similar, narrow distribution of petal sizes despite slightly differing means, with coefficients of variation of 0.17 and 0.16 (Figure 6; see

Table 2. QTL Analysis

Trait	QTL	Chromosome	Position (cM)	Confidence Interval (cM)	LOD	PVE	a	PSV
Leaf area	LAQTL_1	B	30.30	20.3–43.2	3.60	11.0	−0.87 cm^2	966.67
Leaf length	LLQTL_1	B	30.30	18.3–42.2	5.50	17.0	−0.86 cm	136.51
Leaf width	LWQTL_1	B	31.40	21.3–40.2	5.31	16.6	−0.15 cm	272.73
Petal area (ln)	PAQTL_1	A	14.90	12.9–22.0	8.29	11.6	0.33 mm^2	9.27
	PAQTL_2	B	53.26	40.2–59.5	7.70	10.6	0.31 mm^2	8.71
	PAQTL_3	C	5.70	1.0–9.1	4.40	4.8	0.24 mm^2	6.74
	PAQTL_4	F	15.10	9.0–23.6	13.33	15.5	0.37 mm^2	10.39
	PAQTL_5	F	35.80	32.8–39.8	11.28	17.6	0.38 mm^2	10.67
	PAQTL_6	G	54.10	49.4–58.7	13.78	16.8	0.39 mm^2	10.96
Petal length	PLQTL_1	A	15.90	12.9–21.9	7.06	12.8	0.16 mm	13.33
	PLQTL_2	A	44.20	39.2–53.3	5.12	11.1	0.14 mm	11.67
	PLQTL_3	B	40.23	31.4–62.1	4.00	2.9	0.10 mm	8.33
	PLQTL_4	F	21.60	14.1–27.1	7.92	16.3	0.11 mm	9.17
	PLQTL_5	F	37.80	33.9–42.2	8.03	17.8	0.18 mm	15.00
	PLQTL_6	G	55.10	46.4–63.7	5.98	8.4	0.12 mm	10.00
Petal width	PWQTL_1	A	27.10	13.9–30.7	10.09	15.1	0.11 mm	11.22
	PWQTL_2	B	55.20	39.2–62.1	5.22	7.6	0.08 mm	8.16
	PWQTL_3	C	5.70	3.6–8.1	7.33	10.1	0.10 mm	10.20
	PWQTL_4	C	71.80	61.4–71.8	4.81	7.0	0.07 mm	7.14
	PWQTL_5	F	15.10	9–23.6	6.85	9.2	0.08 mm	8.16
	PWQTL_6	G	55.10	47.4–62.7	7.79	11.8	0.10 mm	10.20
Distance anthers - stigma	DASQTL_1	B	39.20	30.3–48.7	3.25	7.2	0.06 mm	12.63
	DASQTL_2	D	27.80	22.8–32.8	7.61	17.8	0.10 mm	21.05
	DASQTL_3	G	36.00	32.7–46.4	4.39	12.6	0.09 mm	18.95
Petal opening angle	POAQTL_1	B	33.43	20.3–40.2	4.04	18.3	3.1°	29.88
	POAQTL_2	D	29.80	26.8–33.8	8.40	23.3	4.7°	45.30
	POAQTL_3	F	39.90	34.8–44.1	5.16	20.2	3.1°	29.88

PVE, percentage of total genetic variation explained; a, additive genotypic effect (positive value means *C. grandiflora* allele increases phenotypic value by the stated value); PSV, percentage of species variation explained (see Methods). Confidence interval represents the region on the genetic map surrounding the QTL peak in which the LOD score is less than two units below the maximum LOD value of the QTL peak.

Supplemental Table 5 online). The progeny of the crosses between either of the *C. rubella* accessions and *C. grandiflora* Cg926 produced a much wider phenotypic distribution, spanning either the full range between the parental strains (Cr1377, coefficient of variation 0.34) or a large part of it (Cr1504, coefficient of variation 0.26). By contrast, the distribution of petal sizes in the F2 of the cross between the two *C. rubella* accessions was as narrow as that in the two parental strains (coefficient of variation 0.17), with the mean intermediate between that of the two parents. Variation in petal opening angle in the parental *C. rubella* strains was similarly distributed, with coefficients of variation of 0.18 and 0.14. Whereas in the progeny of crosses between either the *C. rubella* accession and *C. grandiflora* Cg926 the average petal opening angle was larger, the coefficients of variation were very similar to those seen in the *C. rubella* parents (0.15 and 0.17). The distribution of opening angles in the F2 progeny from crossing the two *C. rubella* strains did not differ from that in the parents regarding the mean. However, we found several individuals (6 out of 184) with a petal angle exceeding 50°, the maximum value observed in the parental strains, resulting in a higher coefficient of variation (0.23).

To test whether these increased opening angles were heritable, we tested the progenies of four F2 individuals each from the center of the phenotypic distribution (with opening angles between 33.4° and 40.9°) and from the high end of the distribution (with opening angles between 50.4° and 65.0°). However, the progenies of these two groups did not differ in their distributions of petal opening angles (see Supplemental Figure 6 online), suggesting that the higher-than-parental phenotype values in the F2 were not stably inherited, arguing for environmental or random effects in the F2. Thus, there is no evidence for transgressive segregation of petal size or petal opening angle in the cross of two distantly related *C. rubella* accessions, suggesting that the mutations that have reduced petal size and opening angle in these two accessions relative to *C. grandiflora* affect the same genetic loci. This lack of transgressive segregation strongly argues against the notion that petal size and petal opening were reduced by mutations of different genetic loci in local populations of *C. grandiflora*. Distinguishing whether petal size and opening were already reduced before the geographical spread of *C. rubella* or independently after the spread (but involving mutations in the same genetic loci in both tested *C. rubella* accessions) will require a molecular definition of the causal mutations underlying the reduced petal size and opening in *C. rubella*.

Adaptive Significance of the Selfing Syndrome in *C. rubella*

The observation that independently evolved selfing lineages frequently show the same morphological alterations in their flowers
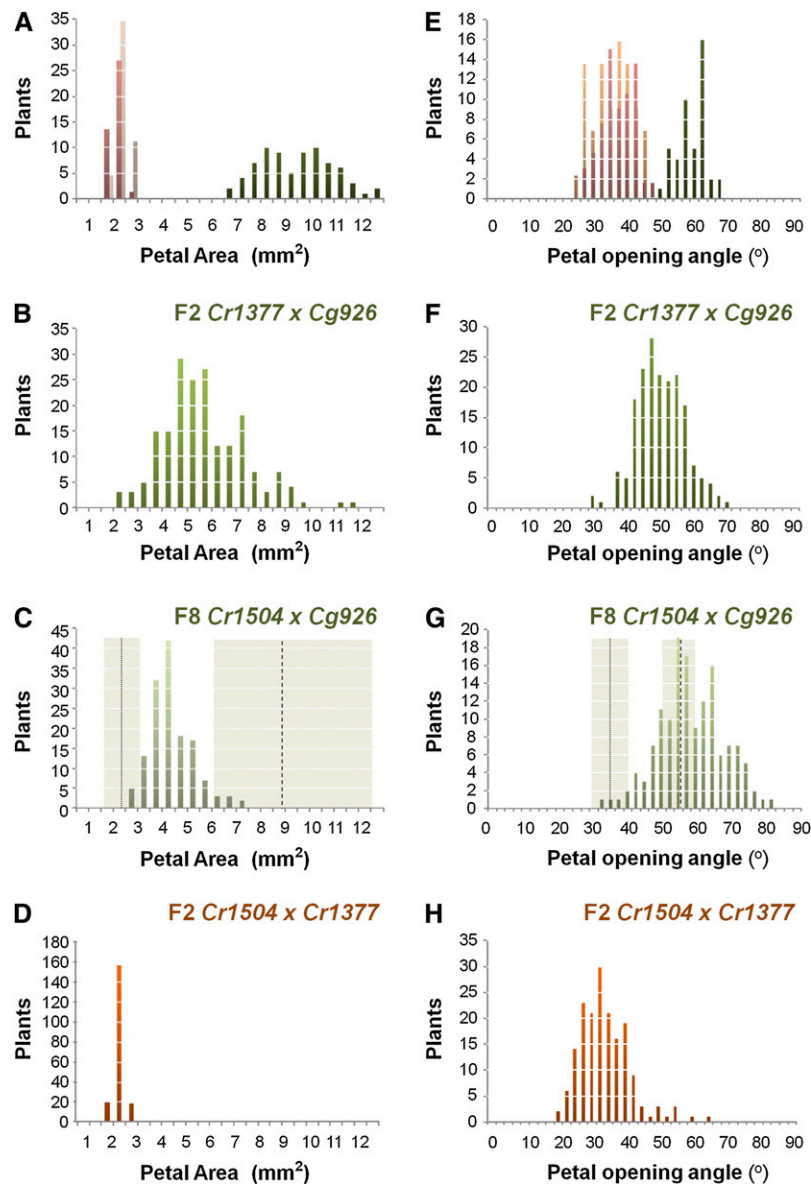
Figure 6. Distribution of Petal Sizes and Petal Opening Angles in Crosses Involving Different *C. rubella* Accessions.

(A) to **(H)** Frequency histograms of petal sizes (**[A]** to **[D]**) and petal opening angles (**[E]** to **[H]**) in the indicated populations.

(A) and **(E)** The two *C. rubella* accessions used (Cr1377 and Cr1504; red/brown tones) compared with *C. grandiflora* accession Cg926 (green).

(B) and **(F)** F2 population from the cross *C. rubella* Cr1377 × *C. grandiflora* Cg926.

(C) and **(G)** F8 RIL population from the cross *C. rubella* Cr1504 × *C. grandiflora* Cg926. The mean values of the phenotypic trait of the two parents *C. rubellla* Cr1504 (dotted line) and *C. grandiflora* Cg926 (dashed line) are shown. Their respective standard deviations are indicated by the shaded gray areas.

(D) and **(H)** F2 population from the intercross between the two *C. rubella* accessions Cr1377 × Cr1504.

compared with their outbreeding ancestors suggests that these alterations are of adaptive significance. However, our knowledge about what drives the evolution of the selfing syndrome is limited. One hypothesis is that the morphological changes in the flowers of selfing species increase the efficiency of self-pollination relative to what could be achieved in self-compatible plants with a floral morphology of their outbreeding ancestors. To test this hypoth-

esis, we introgressed the S-locus from *C. rubella* accession 1504 into *C. grandiflora* accession 926 by six rounds of backcrossing. Petal size and flower opening in the resulting BC6F1 plants are very similar to *C. grandiflora* (Figures 7B and 7C), yet the plants are fully self-compatible. When manually selfed, these plants produced very similar numbers of developing seeds as did self-incompatible *C. grandiflora* plants from the parental accession

Cg926 after cross-pollination (Cg926, 19.8 ± 4.8 [mean ± SD]; Cg-SC1, 17.0 ± 1.8; Cg-SC2, 19.3 ± 1.3). Thus, they likely resemble the plants after the breakdown of self-incompatibility in a *C. grandiflora*–like ancestor.

We used these plants to estimate the efficiency of autogamous self-pollination compared with that in current *C. rubella* individuals. To do so, we calculated the ratio between the number of seeds set by unmanipulated flowers and the number of seeds after manual self-pollination, thus excluding possible differences in ovule number per flower. The selfing ratio estimated in the self-compatible *C. grandiflora* introgression lines was only half that in *C. rubella* individuals, indicating that flowers of the latter are better adapted to highly efficient self-pollination than the flowers of their hypothetical early ancestors (Figure 7A). To determine the contribution of individual floral traits (PA, PL, PW, DAS, and POA) to the more efficient self-pollination in *C. rubella*, we looked for correlations between these traits and the selfing efficiency in a subset (46) of our RILs. Although the selfing efficiency tended to decrease with increasing petal size, as well as with an increased distance between anthers and stigma, only the negative correlation between POA and the selfing efficiency retained statistical significance after correcting for multiple testing (Figure 7D). Thus, flowers of *C. rubella* are adapted to highly efficient self-pollination, and in particular the reduction in the opening of the petals and the flower as a whole may have been directly selected for because of its positive effect on efficient self-pollination.

DISCUSSION

In this study, we characterized the developmental and genetic basis of critical selfing-syndrome traits in *Capsella*. In addition, we have begun to address the evolutionary history of the flower-size reduction in the lineage leading to *C. rubella* and the potential adaptive value of the reduced flowers.

Developmental Basis of the Altered Flower Morphology in *C. rubella*

The changes to flower morphology in the *C. rubella* lineage compared with *C. grandiflora* are highly specific in that leaf traits such as length, width, and area do not differ much between the two species. This is remarkable when considering that most mutants with altered organ size identified from mutagenesis screens in *Arabidopsis* or *Antirrhinum majus* show changes to both leaf and floral organ sizes (Breuninger and Lenhard, 2010). These general growth effects indicate that the developmental-genetic factors that control organ growth are largely shared between leaves and the homologous floral organs. Exceptions to this general rule exist, such as mutations in *BIGPETAL*, *BIG BROTHER*, and *JAGGED* (*JAG*), which strongly affect the size of floral organs but minimally change leaf size (Dinneny et al., 2004; Disch et al., 2006; Szécsi et al., 2006). Thus, in principle, the size changes in *C. rubella* flowers might be specific because the causal mutations all affect such factors with a predominant effect only on flowers. In fact, the *Capsella JAG* homolog (corresponding to marker B07) is located in the confidence interval for PAQTL_2. As *JAG* is required to prevent a premature arrest of

cell proliferation in *Arabidopsis* petals, a mutation in the *C. rubella JAG* ortholog could plausibly underlie the shortened period of cell proliferation. Sequencing the alternative alleles in our population predicted several amino acid exchanges in the *Capsella JAG* homolog between the two parents (see Supplemental Figure 7 online), yet the functional significance of these changes is currently unknown. An alternative explanation could be that, in contrast with the coding-sequence mutations that underlie the organ-size phenotypes in model species, the differences between *C. grandiflora* and *C. rubella* flowers are mainly due to *cis*-regulatory changes that alter the expression of shared growth regulators specifically in flowers.

Developmentally, the difference in final petal size between the two *Capsella* species is caused by a reduced period of proliferative growth in *C. rubella*, whereas the rate of growth is unchanged. How does this compare with the patterns of developmental changes that have been found when comparing flower growth between other related outbreeding and selfing taxa (Guerrant, 1988; Fenster et al., 1995; Runions and Geber, 2000)? In *C. xantiana*, *Mimulus*, or *Limnanthes*, the growth phase has been shortened, but the rate of growth has increased in the selfing compared with the outbreeding taxa (Guerrant, 1988; Fenster et al., 1995; Runions and Geber, 2000); in *A. uniflora*, the converse is true (i.e., the rate of growth is reduced but the growth phase extended in the selfers) (Hill et al., 1992). Thus, although there has been no increase in the rate of petal growth in *C. rubella*, our results resemble the developmental changes found in *Clarkia*, *Mimulus*, and *Limnanthes*. This pattern has been interpreted in support of the hypothesis that selfing in these taxa evolved as a by-product of selection for rapid maturation in marginal habitats. However, for *C. rubella*, the lack of a systematic difference in flowering time, overall rate of development, and plant stature between *C. grandiflora* and *C. rubella* accessions argues against this notion.

Genetics of Selfing-Syndrome Traits

Our QTL analysis indicates a complex genetic basis for the evolution of the two selfing-syndrome traits under study. The distributions of phenotypes in the RIL population are gradual for both petal size and flower-opening traits.

For petal size, few individuals show the extreme values of either parents, indicating the involvement of a substantial number of contributing loci. Overall, the distribution is shifted toward lower phenotypic values; however, there was no evidence for dominance of the *C. rubella* alleles at petal size QTL from the F1 plants analyzed. Also, the F2 population of an independent *C. grandiflora* × *C. rubella* cross shows a distribution of petal sizes centered around the arithmetic mean of the two parents (i.e., shifted toward higher values compared with the RIL population). Thus, a likely explanation for the smaller average petal size in the RILs is inadvertent selection against *C. grandiflora* alleles at petal-size QTL because of their linkage with genomic regions showing segregation distortion in the RILs; the petal-size QTL on chromosome A is linked to a deleterious recessive mutation in the *C. grandiflora* background that causes a light green appearance of leaves and slow growth, whereas the petal-size QTL on chromosome G is linked to the *C. grandiflora* S-locus allele.
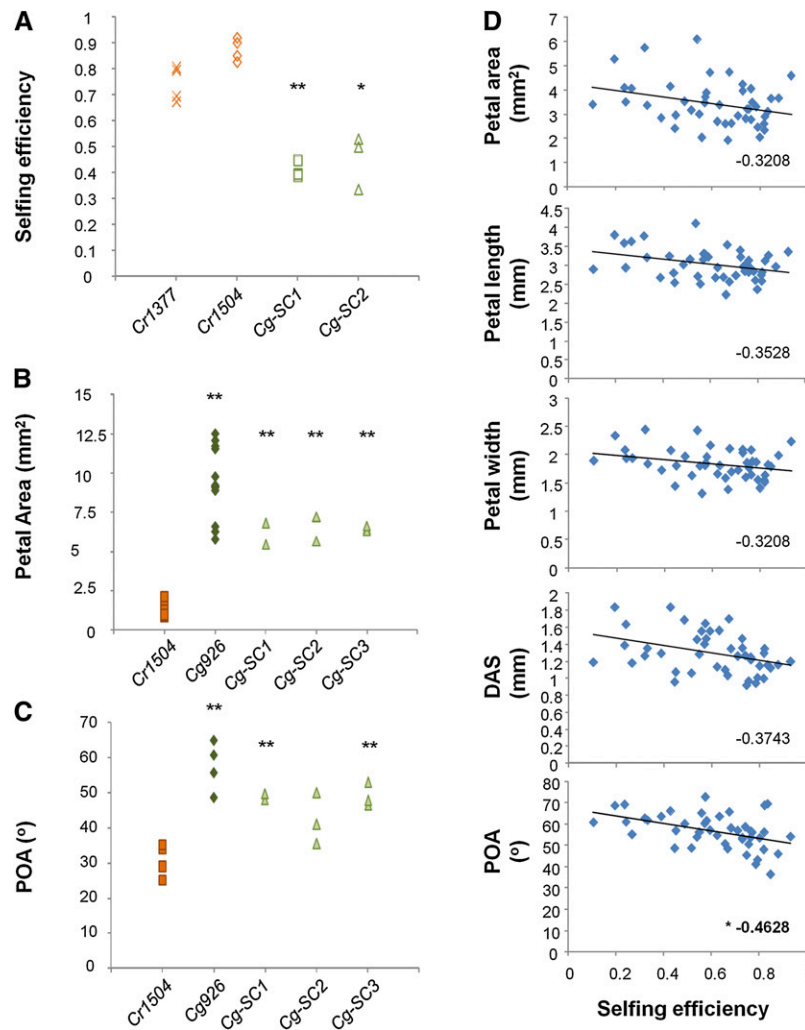
Figure 7. Flower Morphology and the Efficiency of Self-Pollination.

(A) Efficiency of self-pollination in two *C. rubella* accessions (Cr1377, orange crosses; Cr1504, orange diamonds) and in two independently derived self-compatible *C. grandiflora*–like lines (Cg-SC1 and Cg-SC2, light-green squares and triangles, respectively). Each data point is the value from one individual plant.

(B) and **(C)** Comparison of flower morphology between *C. rubella* (Cr1504, orange squares), *C. grandiflora* (Cg926, dark-green diamonds), and three self-compatible *C. grandiflora*–like lines (Cg-SC1, Cg-SC2, and Cg-SC3, light-green triangles). Each data point is the average value of two mature flowers.

(B) Petal area.

(C) Petal opening angle. Asterisks indicate statistically significant differences from *C. rubella* Cr1504 as determined by a Student's *t* test with Bonferroni correction at $P < 0.05$ (*) and $P < 0.01$ (**).

(D) Correlation plots of selfing efficiency and the indicated phenotypic parameters measured in the RIL population. For each pairwise comparison, dots represent individual RIL lines, and the dark line represents the linear-regression line. Values shown are Pearson's correlation coefficients (*r*), with significant correlations ($P < 0.05$) indicated by bold type and an asterisk.

[See online article for color version of this figure.]

Notably, for each of the floral-trait QTL, the *C. grandiflora*–derived allele increased the phenotype value. At present, this is difficult to reconcile with the observed transgressive segregation for POA and DAS. The latter could either be due to the action of several undetected small-effect QTL, or it might reflect environmental variation that was not controlled for. Also, we note that although the *Capsella* system could in principle be used to test

predictions from evolutionary theory about the dominance behavior of selected alleles (Charlesworth, 1992), our RIL design precludes the estimation of dominance coefficients for the QTL because of the homozygosity of the lines.

The numbers of QTL that we identified as influencing the different traits only represent minimum estimates because of the limited number of RILs that we were able to establish, reducing

the power of QTL mapping. Despite this limitation, we detected at least eight significant QTL influencing aspects of petal size and four QTL for aspects of flower opening. Thus, the evolution of these selfing-syndrome traits in *C. rubella* has involved mutations to numerous genes, suggesting that it has occurred in a stepwise manner.

In agreement with previous comparative QTL mapping studies for leaf and floral traits (Frary et al., 2004; Juenger et al., 2005), the single leaf-size QTL we detected did not overlap with any of the loci found to influence petal growth. Also, there was no genetic correlation between leaf and petal size in our population. Together, these observations support the notion that natural phenotypic variation in leaves and petals is frequently under the control of distinct genetic modules, despite the homology of the organs (cf. above).

Evolutionary History of Flower Size Reduction in *C. rubella*

The transition to selfing in *Capsella* was associated with a severe population bottleneck in the lineage leading to *C. rubella* (Foxe et al., 2009; Guo et al., 2009). All of the studied accessions of *C. rubella* show strongly reduced flower size and flower opening typical of selfing species, whereas no such variation was observed within *C. grandiflora*. The wide geographical distribution of *C. rubella* raises the question when the selfing syndrome evolved relative to the population growth and geographical spread of the selfer. In an F2 population derived from a cross of two distantly related *C. rubella* accessions, we find no evidence of transgressive segregation for petal size or for flower opening compared with the two parental strains. This suggests that relative to *C. grandiflora* the same loci have been mutated in the two *C. rubella* accessions to reduce petal size and opening.

Thus, it appears either that these traits had already been reduced in the common ancestor of the two tested *C. rubella* accessions or that the evolution of petal size and opening is highly constrained, such that the same loci have been modified during the independent reduction of both in the different *C. rubella* accessions. Given the large number of factors that have already been described as influencing organ growth in genetic model species and that could conceivably be targeted for evolutionary modification, we consider the former explanation as more likely, arguing for a single origin of the smaller, less open flowers. At present (without knowing some of the causal mutations involved), we cannot determine when flowers were reduced relative to the breakdown of self-incompatibility. However, the hypothesis that selfing in *Capsella* arose as a means of ensuring efficient reproduction despite pollinator and/or mate limitation (Foxe et al., 2009; Guo et al., 2009) predicts the breakdown of self-incompatibility as the most plausible first evolutionary step followed by a reduction in flower size, as the latter should be unfavorable in a self-incompatible population already having insufficient levels of cross-pollination.

Adaptive Value of the Selfing Syndrome

At least four not mutually exclusive hypotheses have been proposed to explain the frequent parallel evolution of the selfing syndrome in flowering plants (Sicard and Lenhard, 2011). First,

the reduced floral size and display may result from the reallocation of limited resources away from the now unnecessary tasks of pollinator attraction to other functions; second, selection may have been mainly for an increased efficiency of self-pollination; third, the reduced floral size could be a byproduct of selection for rapid maturation at the whole-plant and the flower level; and fourth, flower size and conspicuousness (including flower opening) may have been reduced to avoid herbivory on large, showy flowers. Here, we tested specifically the hypothesis that the flowers of modern *C. rubella* are more efficient at self-pollinating than those of the presumed earliest ancestor of the *C. rubella* lineage immediately after the breakdown of self-incompatibility, which we assume to have resembled modern *C. grandiflora* in floral morphology (see above). Our results indicate that the efficiency of selfing in this hypothetical ancestor would have been substantially lower than that seen in modern *C. rubella*. To determine which of the individual selfing-syndrome traits contribute to an increased efficiency of self-pollination, we analyzed the selfing rate in a subset of the phenotyped RILs. Only the petal opening angle was significantly negatively correlated with the selfing rate, although the other traits (petal area and anther-stigma distance) also showed similar but weaker trends. Thus, in the case of *Capsella*, the evolution of the selfing syndrome in flowers seems to have been driven at least in part by selection for more efficient self-pollination, potentially to provide reproductive assurance under conditions of pollinator and/or mate limitation after the last ice age.

METHODS

Plants Materials, Growth Conditions, and Generation of RILs

This study used *Capsella rubella* and *Capsella grandiflora* accessions collected at diverse locations within Europe and South America (including kind gifts from Tanja Slotte; Foxe et al., 2009; Guo et al., 2009). Details of the geographical origins are given in Supplemental Table 1 online. Plants were grown under a long-day photoperiod (16 h light/8 h dark) at temperatures of 21°C (day)/16°C (night) and in 70% humidity with a light level of 150 μmol m^{-2} s^{-1}.

RILs were generated by crossing *C. rubella* accession Cr1504 (as male parent) to *C. grandiflora* accession Cg926 (as female parent). One fertile F1 plant was allowed to self. Two hundred and fifty F2 plants were grown up and propagated for an additional six generations by selfing and single-seed descent. A resulting set of 142 F8-RILs were used in this study.

In parallel, self-compatible *C. grandiflora*–like plants, termed *Cg-SC*, were generated by introgressing the *C. rubella* S-locus into a *C. grandiflora* background. To this end, self-fertile F2 plants from the above population were backcrossed to Cg926 six times, always selecting for phenotypic self-compatibility, which is most likely due to the combination of the nonfunctional S-locus allele from *C. rubella* and a weak S-locus allele from *C. grandiflora*. The F1 progeny of the last backcross (the BC6F1 population) were directly used for morphological measurements.

An intraspecific F2 population was generated by crossing two *C. rubella* accessions, Cr1377 (from Argentina) and Cr1504 (Canary Island, La Palma, Spain), belonging to two different early diverging lineages based on the population structure of the species previously described (Foxe et al., 2009). For comparison, a second interspecific F2 population was constructed by pollinating *C. grandiflora* Cg926 with pollen from *C. rubella* Cr1377. The success of crossing was confirmed in the F1 by sequencing, and the hybrids were propagated to the F2 or F3 (for progeny testing of selected F2 individuals for petal opening angle) generations for further analysis.

Construction of the Genetic Map

C. rubella genomic DNA was digested with *Hind*III, cloned into pBluescript II KS– (Fermentas) before being sequenced. Polymorphisms were identified by sequencing fragments of genomic DNA from *C. rubella* accession Cr1504 and from a pool of F2 plants from the cross Cr1504 × Cg926. Primers for sequencing (see Supplemental Table 3 online) were designed either on the basis of the previously determined *C. rubella* genomic sequences or based on *Arabidopsis thaliana* coding sequences. These sequences were selected to be equally distributed all along the *Capsella* genome according to the previously described colinearity between the *Capsella* and *Arabidopsis* genome (Boivin et al., 2004). Sequence alignments and polymorphism detection were performed using the VectorNTI package (Invitrogen), resulting in the 98 polymorphisms presented in Supplemental Table 2 online. These polymorphisms were converted into PCR-based markers (derived cleaved amplified polymorphic sequence [dCAPS] or cleaved amplified polymorphic sequence) using dCAPS finder 2.0 (http://helix.wustl.edu/dcaps/dcaps.html), resulting in the markers given in Supplemental Table 3 online.

The 142 RILs were genotyped with these PCR-based markers. The combinations of primers described in Supplemental Table 3 online were used to amplify genomic DNA of a pool of F8 plants for each RIL. Restrictions of the resulting PCR products with the corresponding enzyme (see Supplemental Table 3 online), and electrophoreses on 3% agarose gels were then employed to reveal the polymorphisms. Linkage groups and the position of each marker were estimated from the observed recombination frequency using the Kosambi mapping function (Kosambi, 1944) in Joint Map 3.0 software (Van Ooijen and Voorrips, 2001). As parameters, we used a LOD grouping of 3.5, a stringency of LOD > 1.0, and REC < 0.40 (Van Ooijen and Voorrips, 2001).

Morphological Measurements

To compare the species-wide phenotypes of *C. rubella* and *C. grandiflora*, five replicate plants of each of the accessions listed in Supplemental Table 1 online were used. For the QTL analysis, 10 F9 plants per RIL were grown under the conditions described above. Position effects in the growth chamber were removed by distributing the replicate plants randomly within the chamber (http://www.random.org/). Phenotypes of F1 and F2 plants from crosses between other *Capsella* accessions were measured from five replicate plants for the F1 generations, whereas no within-genotype replication is possible in the F2. For the Cg-SC introgression lines, three replicate plants were used for each of three independent introgression lineages.

Leaf size was measured on fully expanded 5th leaves, whereas petal size was measured from the 5th and 6th fully open flowers on the main inflorescence. Area, width, and length were measured using ImageJ (http://rsbweb.nih.gov/ij/) from digital images of dissected organs.

To determine the efficiency of self-pollination in the RILs, two fully open flowers per plant were manually self-pollinated on 10 replicate plants of 46 RILs. Two weeks later, siliques formed by these flowers and siliques formed by the two next unmanipulated flowers were collected to count seeds and record the mating system of the plants (self-compatible or self-incompatible). For each plant, the ratio of the average number of seeds in self-pollinated flowers versus the maximum number of seeds from the manually selfed flowers was used to estimate the efficiency of self-pollination. Self-incompatible plants were removed from the latter analysis. For the Cg-SC introgression lines, three replicate plants were used for each of two independent introgression lineages.

Kinetic analysis of petal development was performed as described (Disch et al., 2006). Briefly, two developing petals per flower bud were manually dissected and measured, starting with the oldest unopened flowers and extending to the youngest bud from which petals could still be dissected. A total of 38 unopened flower buds were dissected from each

of five individuals of *C. grandiflora* accession Cg926 and 25 buds each from five individuals of *C. rubella* accession Cr1504. The plastochron (time interval between the formation of two successive flowers) was calculated from the number of flowers opening up within 7 d.

Average adaxial petals cell size was estimated as the ratio of cell number per unit area. Petals were incubated overnight in 70% ethanol before microphotographing.

Flower architecture (distance between anthers and stigma; ratio of the length of the long stamens to the length of the gynoecium; petal opening angle) was quantified from photographs of dissected flowers. From these, one lateral sepal and one petal had been removed to visualize the central organs of the flower before photographing the flower from the top and the side, with the adaxial sepal to the right. The flowers were between the 10th and the 15th flower of the main inflorescence. Here, only five replicate plants were used for both the RILs and the accessions. Parameters were measured from the digital photographs using ImageJ, taking measurements involving two different stamens or petals per flower and using the average value.

Statistical Analysis

Statistical analyses were performed in Genstat 11.0 (http://www.vsni.co.uk/software/genstat/).

The statistical significance of all phenotypic differences was assessed by two-tailed Student's *t* tests. The null hypothesis was rejected at $P < 0.05$. The significance level at which the null hypothesis could be rejected is denoted on each figure by the number of asterisks, with $P < 0.05$ (*), $P < 0.01$ (**), and $P < 0.001$ (***).

Variance components of the traits investigated were estimated by unbalanced analysis of variance and used to calculate the broad sense heritability (H^2) as the ratio of the variance among the RILs (Vg = [global variance − variance within RILs (Ve)]/ number of replicates per RIL) divided by the total phenotypic variance. As a relative indicator of dispersion, we calculated the coefficient of genetic variance (CVg) as the ratio of the standard deviation (square root of the among-RILs variance) to the mean of the corresponding trait over all RILs (m): $CVg = (Vg^{1/2}/m) \times 100$.

Genetic correlations between traits were estimated using Pearson's correlation coefficient *r* (function Correlation in Genstat 11.0) with a two-sided test of significance. Within each set of comparisons, the P values were adjusted for multiple testing using Bonferroni correction (Rice, 1989).

The normality of the trait data distributions was tested using Shapiro-Wilk, Anderson-Darling, Lilliefors, and Jarque-Bera tests (Anderson and Darling, 1952; Shapiro and Wilk, 1965; Lilliefors, 1967; Jarque and Bera, 1987). The null hypothesis that a sample set came from a normally distributed population was rejected at $P < 0.05$ in all the different tests used. To compare the segregation of selfing syndrome traits in the descendants of our intra- and interspecific crosses, we determined their distribution parameters. For each data set, we calculated the mean, median, variance, standard deviation, maximum, and minimum values. The range was determined by subtracting the minimum from the maximum value. The coefficient of variation corresponds to the standard deviation divided by the corresponding mean. As an indicator of asymmetry, we calculated the skewness coefficient of each distribution using the SKEW function in Excel 2007 (Microsoft). Finally, the means of the data sets were compared by Student's *t* test and considered different at $P < 0.05$.

Mapping of QTL

QTL mapping was performed using MAPQTL 4.0 (Van Ooijen et al., 2000) using phenotypic mean values of the RILs. The following iterative protocol was used for all traits. Preliminary interval mapping was performed to define cofactors (markers surrounding the QTL). These cofactors were

submitted to the automated cofactor selection function of MAPQTL to retain only significant cofactors. These were then used for a restricted multiple-QTL scan to estimate for each QTL the maximum LOD, the additive genotypic effect (a), and the proportion of the total variance explained. This method uses multiple QTL mapping to test for the presence of QTL by considering the effect of other segregating QTL (defined by cofactors). To reduce the risk of false positive detection of QTL, we used restricted analyses excluding linked cofactors. Genome-wide permutation tests (10,000 permutations) were used to obtain LOD score significance thresholds. The 95% confidence intervals for the location of the QTL were determined based on a two-LOD support interval (Van Ooijen, 1992). LOD score peaks on the same linkage group were interpreted as representing different QTL if the 2-LOD confidence intervals of the peaks did not overlap. The percentage of species variation explained was calculated by dividing the absolute value of 2a by the difference of the means of the two species (*C. grandiflora* and *C. rubella*) for the corresponding trait.

RT-PCR

Total RNA was extracted from pooled inflorescences of *C. rubella* and *C. grandiflora* with young flower buds, treated with TURBO DNase (Ambion), and reverse transcribed with SUPERSCRIPT III reverse transcriptase (Invitrogen) and oligo(dT) primer according to the manufacturers' recommendations. The putative *JAG* homolog was amplified using the primers JAG ORF_F (5′-ATGAGGCATGAGGAGAATTACTTAGACCT-3′) and JAG REV (5′- GATGATCTTGAAACCGATTGATGGGGAA-3′) and the *Capsella* ortholog of *PDF2* with the primers PDF2-qPCRfor2 (5′-TGGCTCCA-GTCTTGGGTAAG-3′) and PDF2-qPCRrev2 (5′-GCCTGTCTTCAGCAA-GTTCTAC-3′). Levels of the RT-PCR products were compared visually after agarose gel electrophoresis and ethidium bromide staining.

Accession Numbers

Accession numbers for *C. grandiflora* accessions used are Cg103.11, Cg5a, Cg83.19, Cg88.12, Cg89.13, Cg91.17, Cg926.11, Cg93.2, and Cg94.16. Accession numbers for *C. rubella* accessions used are 1504, TAAL-1-TS3, GÖ665-1, 1GR1-TS1, 22.5, 23.9, 27.2, 34.11, 39.1-TS1, Cr86IT1-C, 4.23, 1209/26-TS4, 8.5, 1215/17-TS1, and 1377/5. Please see Supplemental Table 1 online for more details.

Supplemental Data

The following materials are available in the online version of this article.

Supplemental Figure 1. Overall Morphology of *C. grandiflora* and *C. rubella* Accessions.

Supplemental Figure 2. Differences in Sex Allocation between *C. grandiflora* and *C. rubella*.

Supplemental Figure 3. Genetic Mapping of the *Capsella* S-Locus and Segregation Distortion in the RIL Population.

Supplemental Figure 4. Distribution of Phenotypes in the *C. grandiflora* × *C. rubella* RIL Population.

Supplemental Figure 5. Petal Sizes of F1 Hybrids.

Supplemental Figure 6. Petal Opening Angles in F3 *C. rubella* Cr1377 × *C. rubella* Cr1504 Plants.

Supplemental Figure 7. Characterization of the Putative *Capsella* *JAG* Orthologs.

Supplemental Table 1. Geographic Origin of Accessions Used in This Study.

Supplemental Table 2. Polymorphisms Used to Develop PCR-Based Markers and the Corresponding *Arabidopsis* Loci.

Supplemental Table 3. Primer Sequences and Information about PCR-Based Markers.

Supplemental Table 4. Normality Tests for Distributions of Phenotypes in the RIL Population, Accessions, and F2 Populations.

Supplemental Table 5. Statistical Description of Petal Size and Petal Opening-Angle Distributions.

AUTHOR CONTRIBUTIONS

A.S., I.B., and M.L. designed the research. A.S., N.S., K.H., J.D., and M.L. performed research. B.N. contributed novel biological materials. A.S., K.H., and M.L. analyzed the data. A.S. and M.L. wrote the article.

REFERENCES

Anderson, T.W., and Darling, D.A. (1952). Asymptotic theory of certain "goodness-of-fit" criteria based on stochastic processes. Ann. Math. Stat. **23:** 193–212.

Baker, H.G. (1955). Self-compatibility and establishment after 'long-distance' dispersal. Evolution **9:** 347–349.

Barrett, S.C. (2002). The evolution of plant sexual diversity. Nat. Rev. Genet. **3:** 274–284.

Barrett, S.C. (2010). Understanding plant reproductive diversity. Philos. Trans. R. Soc. Lond. B Biol. Sci. **365:** 99–109.

Bernacchi, D., and Tanksley, S.D. (1997). An interspecific backcross of *Lycopersicon esculentum* x *L. hirsutum*: Linkage analysis and a QTL study of sexual compatibility factors and floral traits. Genetics **147:** 861–877.

Boivin, K., Acarkan, A., Mbulu, R.S., Clarenz, O., and Schmidt, R. (2004). The Arabidopsis genome sequence as a tool for genome analysis in Brassicaceae. A comparison of the Arabidopsis and *Capsella rubella* genomes. Plant Physiol. **135:** 735–744.

Breuninger, H., and Lenhard, M. (2010). Control of tissue and organ growth in plants. Curr. Top. Dev. Biol. **91:** 185–220.

Busch, J.W., and Schoen, D.J. (2008). The evolution of self-incompatibility when mates are limiting. Trends Plant Sci. **13:** 128–136.

Charlesworth, B. (1992). Evolutionary rates in partially self-fertilizing species. Am. Nat. **140:** 126–148.

Chen, K.Y., Cong, B., Wing, R., Vrebalov, J., and Tanksley, S.D. (2007). Changes in regulation of a transcription factor lead to autogamy in cultivated tomatoes. Science **318:** 643–645.

Darwin, C. (1876). The Effects of Cross and Self Fertilisation in the Vegetable Kingdom. (London: John Murray).

Dinneny, J.R., Yadegari, R., Fischer, R.L., Yanofsky, M.F., and Weigel, D. (2004). The role of JAGGED in shaping lateral organs. Development **131:** 1101–1110.

Disch, S., Anastasiou, E., Sharma, V.K., Laux, T., Fletcher, J.C., and Lenhard, M. (2006). The E3 ubiquitin ligase BIG BROTHER controls arabidopsis organ size in a dosage-dependent manner. Curr. Biol. **16:** 272–279.

Fenster, C.B., Diggle, P.K., Barrett, S.C.H., and Ritland, K. (1995). The genetics of floral development differentiating two species of Mimulus (Scrophulariaceae). Heredity **74:** 258–266.

Fishman, L., Kelly, A.J., and Willis, J.H. (2002). Minor quantitative trait loci underlie floral traits associated with mating system divergence in Mimulus. Evolution **56:** 2138–2155.

Foxe, J.P., Slotte, T., Stahl, E.A., Neuffer, B., Hurka, H., and Wright, S.I. (2009). Recent speciation associated with the evolution of selfing in *Capsella*. Proc. Natl. Acad. Sci. USA **106:** 5241–5245.

Frary, A., Fritz, L.A., and Tanksley, S.D. (2004). A comparative study of the genetic bases of natural variation in tomato leaf, sepal, and petal morphology. Theor. Appl. Genet. **109:** 523–533.

Georgiady, M.S., Whitkus, R.W., and Lord, E.M. (2002). Genetic analysis of traits distinguishing outcrossing and self-pollinating forms of currant tomato, *Lycopersicon pimpinellifolium* (Jusl.) Mill. Genetics **161:** 333–344.

German, D.A., Friesen, N., Neuffer, B., Al-Shehbaz, I.A., and Hurka, H. (2009). Contribution to ITS phylogeny of the Brassicaceae, with special reference to some Asian taxa. Plant Syst. Evol. **283:** 33–56.

Goodwillie, C., Ritland, C., and Ritland, K. (2006). The genetic basis of floral traits associated with mating system evolution in Leptosiphon (Polemoniaceae): An analysis of quantitative trait loci. Evolution **60:** 491–504.

Guerrant, E.O. (1988). Heterochrony in plants: The intersection of evolution, ecology, and ontogeny. In Heterochrony in Evolution, M.L. McKinney, ed (New York: Plenum Press), pp. 111–133.

Guo, Y.L., Bechsgaard, J.S., Slotte, T., Neuffer, B., Lascoux, M., Weigel, D., and Schierup, M.H. (2009). Recent speciation of *Capsella rubella* from *Capsella grandiflora*, associated with loss of self-incompatibility and an extreme bottleneck. Proc. Natl. Acad. Sci. USA **106:** 5246–5251.

Hill, J.P., Lord, E.M., and Shaw, R.G. (1992). Morphological and growth rate differences among outcrossing and self-pollinating races of *Arenaria uniflora* (Caryophyllaceae). J. Evol. Biol. **5:** 559–573.

Hurka, H., and Neuffer, B. (1997). Evolutionary processes in the genus *Capsella* (*Brassicaceae*). Plant Syst. Evol. **206:** 295–316.

Jarque, C.M., and Bera, A.K. (1987). A test for normality of observations and regression residuals. Int. Stat. Rev. **55:** 163–172.

Juenger, T., Pérez-Pérez, J.M., Bernal, S., and Micol, J.L. (2005). Quantitative trait loci mapping of floral and leaf morphology traits in *Arabidopsis thaliana*: Evidence for modular genetic architecture. Evol. Dev. **7:** 259–271.

Koch, M.A., and Kiefer, M. (2005). Genome evolution among cruciferous plants: a lecture from the comparison of the genetic maps of three diploid species—*Capsella rubella, Arabidopsis lyrata* subsp. *petraea*, and *A. thaliana.* Am. J. Bot. **92:** 761–767.

Kosambi, D.D. (1944). The estimation of map distance from recombination values. Ann. Eugen. **12:** 172–175.

Lilliefors, H. (1967). On the Kolmogorov–Smirnov test for normality with mean and variance unknown. J. Am. Stat. Assoc. **62:** 399–402.

Lin, J.Z., and Ritland, K. (1997). Quantitative trait loci differentiating the outbreeding *Mimulus guttatus* from the inbreeding M. platycalyx. Genetics **146:** 1115–1121.

Lloyd, D.G. (1992). Self- and cross-fertilization in plants. II. The selection of self-fertilization. Int. J. Plant Sci. **153:** 370–380.

Ornduff, R. (1969). Reproductive biology in relation to systematics. Taxon **18:** 121–133.

Paetsch, M., Mayland-Quellhorst, S., Hurka, H., and Neuffer, B. (2010). Evolution of the mating system in the genus *Capsella* (Brassicaceae). In Evolution in Action: Adaptive Radiations and the Origins of Biodiversity, M. Glaubrecht and H. Schneider, eds (Berlin: Springer-Verlag), pp. 77–100.

Paetsch, M., Mayland-Quellhorst, S., and Neuffer, B. (2006). Evolution of the self-incompatibility system in the Brassicaceae: Identification of S-locus receptor kinase (SRK) in self-incompatible *Capsella grandiflora*. Heredity **97:** 283–290.

Rice, W.R. (1989). Analyzing tables of statistical tests. Evolution **43:** 223–225.

Runions, C.J., and Geber, M.A. (2000). Evolution of the self-pollinating flower in *Clarkia xantiana* (Onagraceae). I. Size and development of floral organs. Am. J. Bot. **87:** 1439–1451.

Schranz, M.E., Lysak, M.A., and Mitchell-Olds, T. (2006). The ABC's of comparative genomics in the Brassicaceae: Building blocks of cruciferous genomes. Trends Plant Sci. **11:** 535–542.

Shapiro, S.S., and Wilk, M.B. (1965). An analysis of variance test for normality (complete samples). Biometrika **52:** 591–611.

Sen, S., Satagopan, J.M., Broman, K.W., and Churchill, G.A. (2007). R/qtlDesign: Inbred line cross experimental design. Mamm. Genome **18:** 87–93.

Sicard, A., and Lenhard, M. (2011). The selfing syndrome: A model for studying the genetic and evolutionary basis of morphological adaptation in plants. Ann. Bot. (Lond.) **107:** 1433–1443.

Stebbins, G.L. (1950). Variation and Evolution in Plants. (New York: Columbia University Press).

Stebbins, G.L. (1974). Flowering Plants: Evolution above the Species Level. (Cambridge, MA: Belknap Press).

Szécsi, J., Joly, C., Bordji, K., Varaud, E., Cock, J.M., Dumas, C., and Bendahmane, M. (2006). BIGPETALp, a bHLH transcription factor is involved in the control of Arabidopsis petal size. EMBO J. **25:** 3912–3920.

Tanksley, S.D. (1993). Mapping polygenes. Annu. Rev. Genet. **27:** 205–233.

Van Ooijen, J.W. (1992). Accuracy of mapping quantitative trait loci in autogamous species. Theor. Appl. Genet. **84:** 803–811.

Van Ooijen, J.W., Boer, M.P., Jansen, R.C., and Maliepaard, E. (2000). MapQTL (R) 4.0, Software for the Calculation of QTL Positions on Genetic Maps. (Wageningen, The Netherlands: Plant Research International).

Van Ooijen, J.W., and Voorrips, R.E. (2001). JoinMap (R) 3.0, Software for the Calculation of Genetic Linkage Maps. (Wageningen, Netherlands: Plant Research International).

This information is current as of October 30, 2011

Supplemental Data	**http://www.plantcell.org/content/suppl/2011/09/15/tpc.111.088237.DC1.html**
References	This article cites 40 articles, 10 of which can be accessed free at: http://www.plantcell.org/content/23/9/3156.full.html#ref-list-1
Permissions	https://www.copyright.com/ccc/openurl.do?sid=pd_hw1532298X&issn=1532298X&WT.mc_id=pd_hw1532298X
eTOCs	Sign up for eTOCs at: http://www.plantcell.org/cgi/alerts/ctmain
CiteTrack Alerts	Sign up for CiteTrack Alerts at: http://www.plantcell.org/cgi/alerts/ctmain
Subscription Information	Subscription Information for *The Plant Cell* and *Plant Physiology* is available at: http://www.aspb.org/publications/subscriptions.cfm